Korean J. Chem. Eng., 33(6), 1831-1836 (2016)
DOI: 10.1007/s11814-016-0030-9

pISSN: 0256-1115
eISSN: 1975-7220

The particle size effect of N-doped mesoporous carbons as oxygen reduction reaction catalysts for PEMFC

Ulziidelger Byambasuren, Yukwon Jeon, Dorjgotov Altansukh, Yunseong Ji, and Yong-Gun Shul†

Department of Chemical Engineering, Yonsei University, Yonsei-ro 50, Seodaemun-gu, Seoul 03722, Korea
(*Received 9 November 2015 • accepted 25 January 2016*)

Abstract−The particle size effect of N-doped mesoporous carbon was investigated for ORR activity in acid condition and for issue of a mass transfer and gas diffusion in PEMFCs. As for a non-Pt ORR catalyst, nitrogen (N)-doped ordered mesoporous carbons (OMCs) with a various particle sizes with the range of the average 20, 45 and 75 μm were synthesized by the precursor of polyaniline for the N/C species, and a mesoporous silica template was used for the physical structure for preparation of nitrogen doped OMCs. The N-doped mesoporous carbons are promoted by a transition metal (Fe) to improve catalytic activity for ORR in PEMFCs. All the prepared carbons were characterized by via scanning electron microscopy (SEM), and to evaluate the activities of synthesized doped carbons, linear sweep was recorded in an acidic solution to compare the ORR catalytic activities values for the use in the PEMFC system. The surface area and pore volume were increased as the particles decreased, which was effective for the mass transfer of the reactant for higher activity at the limiting current regions.

Keywords: N-doped Carbons, Ordered Mesoporous Carbons (OMCs), Particle Size, Oxygen Reduction Reaction (ORR), Polymer Electrolyte Membrane Fuel Cell (PEMFC)

INTRODUCTION

Developing metal-free, carbon-based catalysts to replace platinum-based catalysts for oxygen reduction reactions (ORRs) is an emerging area of research in proton exchange membrane fuel cells (PEMFCs) [1]. Since Pt is a precious metal of low abundance, it is thus of great interest to develop Pt-free cathode catalyst for PEMFC. In addition to the need to improve PEMFC commercialization, the cost of catalytic materials also needs to be reduced. Therefore, the search for non-precious-metal as well as metal-free catalysts has become one of the most active and competitive endeavors in the field of fuel cells [2-9].

Recently, incorporation of heteroatoms (e.g., N, B, and S) on to the carbon supports so as to modify their surface and physicochemical properties has been investigated. Among them, N-doped carbons have received considerable attention because the strong electron donor nature of N should promote enhancement in π bonding, leading to improved stability, electron transfer rate, and hence durability of the carbon supports during electrocatalytic processes [10-12]. Therefore, it is of great importance to explore non-precious ORR electrocatalysts with excellent performance by elaborately designing their porous structure, especially the durability and resistance to the fuel crossover effect. Besides, nitrogen-doped carbon materials possess advantages of excellent electrocatalytic activity, long durability, environmental friendliness and low costs, and have been studied intensively [13]. Various kinds of N-doping structures such as N-doped carbon nanotube [14], N-doped carbon nanofiber [15], N-doped graphene [16], N-doped ordered mesoporous carbon [17], N-doped hierarchically macro/mesoporous carbon [18], and so on, have been reported. Among them, the newly developed N-doped hierarchically macro/mesoporous carbon has been thought to be the more promising and commercially valuable ORR catalyst owing to the integrated macro- and mesoporosities in the same catalyst [19]. Macropores can serve as an electrolyte buffering reservoir to shorten the electrolyte diffusion distances to the interior surfaces, while mesopores can provide a large electro-active surface area of the catalyst to facilitate the rapid transport of ions and/or charges [20,21]. However, either the electrocatalytic activity [19,22] or the durability [18,23] of the available N-doped hierarchically macro/mesoporous carbon materials is still unsatisfactory, probably due to their relatively low specific surface areas and/or less extensive hierarchically porous structure, which need to be improved substantially.

Over the past few decades, tremendous research efforts have been exerted in developing metallic catalysts for ORRs, including M-Nx/C materials (M=Fe, Co, Ni or Mn) [24-28]. Of many different catalysts developed so far, heat-treated nitrogen-coordinated iron on a carbon matrix (Fe/N/C) has been recognized as a promising Pt-free catalyst with potential to match the performance of Pt-based catalysts, although the stability of these novel nonprecious metal catalysts under acidic conditions requires to be improved [25,29]. However, some nitrogen-containing carbon nanostructures also retain a significant ORR activity even after removal of metal components [14,27,30]. These results suggest that metal species (e.g., iron) may not act as an active site but rather facilitate the formation of stable nitrogen sites.

One of the main advantages of the carbon materials is the possibility to control a well-established pore size and develop surface

†To whom correspondence should be addressed.
E-mail: shulyg@yonsei.ac.kr

area. In the PEMFC, while power and energy densities are known to be primarily dependent on the porosity, microstructure, and functional groups of the carbon particles [31]. Based on the previous study about the pore size effect of N-doped mesoporous carbon for ORR activity, the CNx with smaller particle size shows good ORR activity at smaller pore size of around 4 nm [33]. It was found that the particle size can control the total pore structure for a better electrochemical reaction during the PEMFC operation. Therefore, in this study, we investigated the effect of particle size distribution of N-doped mesoporous carbon for PEMFC cathode catalyst. N-doped mesoporous carbon was synthesized by polyacrylonitrile as a carbon and nitrogen precursor by three kinds of silica as hard templates, which have different by particles size with the average particle sizes of 20, 45 and 75 μm. The carbons were evaluated by the PEMFC single cell test to examine these effects.

EXPERIMENTAL

1. Catalyst Preparations

SBA-15 ordered mesoporous silica was prepared by following the procedure of Katiyar [32]. SBA-15 particles were synthesized using the tri-block copolymer P123 (PEO20PPO70PEO20) as a structure directing agent. In a typical synthesis 3 g of P123 was dissolved in 60 ml (1.5 M) HCl. The desired amount of CTAB (0.6 g) and TMB (if needed) was first mixed with 25 ml deionized (DI) water separately, and then the two solutions were mixed thoroughly as 20 ml of ethanol (100%) was added. The amount of TMB added was matched to the P123 used. The resulting solution is referred to as the surfactant solution. 10 ml of TEOS was added dropwise to the surfactant solution, and the mixture was vigorously stirred (~500 rpm) for 45 min at 35 °C. After stirring, the mixture was transferred to a stoppered PTFE bottle and stored under static condition at 75 °C for 10 h and then aged at a selected temperature in the range 80-125 °C. The solid product was washed and filtered with DI water repeatedly and dried at room temperature. The removal of organic template was achieved by calcination in ambient air from room temperature to 550 °C, with a heating rate of 1 °C/min, and a holding time of 6 h at 550 °C. The cooling rate was 5 °C/min. In order to change the particle size of silica, different amount of ethanol was added to solution (20 ml, 30 ml and 40 ml ethanol).

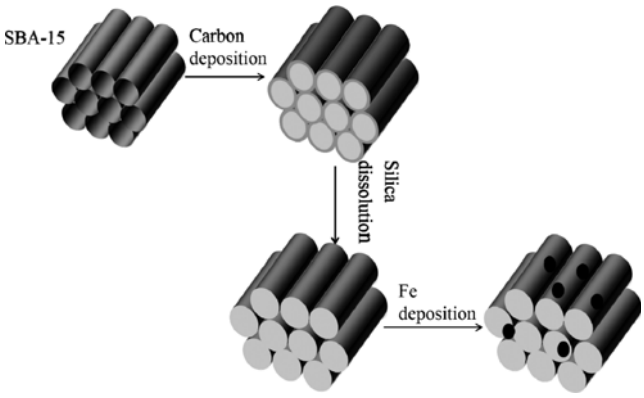

Fig. 1. Schematic drawing of a synthesis procedure of mesoporous carbon catalysts.

The polyaniline (PANI) based ordered mesoporous carbon (OMC) was synthesized with aniline and SBA-15, as shown in Fig. 1. SBA-15 was mixed and then infiltrated with aniline solution in the presence of an azobisisobutyronitrile (AIBN) initiator, through the incipient wetness technique. The mixture was heated at 60 °C for 8 h under static conditions to synthesize a PANI homopolymer through this conventional radical polymerization. Subsequently, the stabilized PANI was carbonized at a temperature of 900 °C in an N_2 atmosphere. OMC was obtained by dissolving the silica template in a 1 M sodium hydroxide aqueous solution at 90 °C. Carbons with various particle sizes (75, 40 and 20 μm) were obtained. The obtained catalysts are named as CNx-A (75 μm), CNx-B (45 μm), and CNx-C (20 μm). The three different of carbons were mixed in the $FeCl_3$ aqueous solution to prepare Fe promoted carbon catalysts. The aqueous suspensions were sonicated and stirred for 3 hours, and then the solvent was removed to a rotary evaporator at 80 °C under vacuum condition. In the second step, heat treatment was carried out in nitrogen at 1,000 °C for 1 hour to produce the catalyst. Carbons were treated with 0.5 M H_2SO_4 at 90 °C for 10 hours to remove the surface deposited iron. Leached catalysts were further heat treated at 800 °C for 1 hour under N 2 flow. The obtained catalysts, these are transition metal promoted, acid leached and heat treated, are named as CNx-A 1.5% Fe-L-HT, CNx-B 1.5% Fe-L-HT and CNx-C 1.5% Fe-L-HT, respectively.

The cathode catalyst ink was prepared by ultrasonically blending the catalyst with a Nafion solution (5 wt%, Alfa Aesar) and isopropyl alcohol for 30 min. The catalyst ink was sprayed onto a gas diffusion layer (GDL) (GDL-10bc) until the desired catalyst loading of 4.95 mg/cm^2 was achieved. The weight percentages of catalyst and Nafion in the dried cathode layer were 50 and 50 wt%, respectively. The anode catalyst was 40 wt% Pt/C, and the Pt loading was 0.5 mg cm^{-2}. The MEA were hot pressed using a Nafion 212 membrane at 120 °C and 1 atm. for 3 min. The geometric area of the MEA was 1 cm^2. The MEA test was carried out in a single cell. Pure H_2 humidified at 75 °C and pure O_2 humidified at 75 °C were supplied to the anode and the cathode, respectively. The flow rates of H_2 and O_2 were 300 and 150 ml min^{-1}, respectively. Polarization experiments were conducted at 75 °C using a fully automated test station without back pressure. The polarization experiments were conducted using an electric load (EL500P, Daegil Electronics) and the AC impedance and CV measurements (0.7 V) results are analyzed using Bio-Logic SAS impedance analyzer (EC-Lab V10.32) PGSTAT-30 (Autolab) to investigate the resistances in the MEAs.

2. Physical Characterizations

The pore sizes and surface area of the synthesized CNx-s were examined by nitrogen adsorption/desorption analysis (data not shown here). The pore size distribution was calculated using the BJH method for mesoporous carbon. SEM images were obtained using JEOL-7001F system. The samples were prepared by placing CNx-s powder on double-sided carbon adhesive tape mounted on the sample holder.

3. RDE and Cyclic Voltammetry Measurements

The RDE measurements involved a Gamry Framework potentiostat/galvanostat in a single-compartment glass cell with a three-electrode arrangement. The glassy carbon electrodes embedded in

Teflon polished with polishing cloth using alumina powder were used as working electrodes for the rotating disk electrode (RDE) measurements. The working electrodes were prepared as follows: in the solution mixture of 1 ml ethanol and 80 µl 5% Nafion, 10 mg sample dispersed. Further, it was sonicated for 3 minutes and stirred for 5 minutes. This procedure was repeated five times. From the suspension, 4 µl was dropped onto the glassy carbon electrode and then dried at room temperature. An RDE experiment was carried out at a scan rate of 5 mV/s within the potential range of +0.8 to −0.2 V in 0.5 M H_2SO_4. Pure O_2 gas was used for the oxygen-saturated electrolyte solution. Commercial Pt/C catalysts (40 wt%) were used for comparison. The loading of Pt/C was the same as like the working electrode. The 10 mg sample was dispersed in a mixture of 1 ml ethanol and 80 µl 5% Nafion solution. It was then sonicated for 3 minutes and stirred for 5 minutes. This procedure was repeated five times. Then 4 µl of this suspension was dropped onto the glassy carbon electrode and then dried at room temperature. A platinum grid was used as the counter-electrode, and a double-junction Ag/AgCl 3M KCl electrode served as the reference electrode.

RESULTS AND DISCUSSION

The particle sizes of N-doped mesoporous carbons were examined by scanning electron microscopy (SEM), as shown in Fig. 2. The synthesized mesoporous carbons were different from each other by the particle size as the different size of silica templates was used by changing the synthesis conditions. The particle sizes of synthesized carbons ranged for 75 µm, 45 µm and 20 µm as displayed in Fig. 3, which is definitely the same as the size of the prepared silica templates.

Table 1. Pore diameter, pore volume and specific area of the SBA-15 silicas and CNx carbons with different particle sizes

Sample	Pore diameter (nm)	Specific surface area (m^2/g)	Total pore volume (cm^2/g)
SBA-15-A	4.66	656.71	0.68
SBA-15-B	4.49	757.38	0.75
SBA-15-C	4.15	822.67	0.85
CNx-A	4.55	629.15	0.73
CNx-B	4.24	704.64	0.75
CNx-C	4.13	822.37	0.85

The pore configuration of the synthesized N-doped mesoporous carbon (CNx-A (75 µm), and CNx-B (45 µm) and CNx-C (20 µm)) catalysts and each silica templates was determined by a multipoint Brunauer Emmett Teller analysis of the nitrogen adsorption/desorption isotherms recorded on the BELSORP surface area analyser. As in Table 1, the silica templates showed an expectable decrease in the pore diameter. On the other hand, the BET surface area largely increased from 656.71 to 822.67 with an increase of the pore volume as well, since the smaller particle provided more surfaces from many pores to adsorb the reactants. After the synthesis of all the CNx series in this study, a similar tendency with no big change in each values was observed for the samples with the particle sizes of 20, 45 and 75 µm, respectively, indicating that well-matched N-doped mesoporous carbons according to the each silica templates were produced. It can be seen that BET surface area of carbons increased from 629.15 to 704.64 and 822.37 m^2/g for the CNx-A, CNx-B and CNx-C, respectively, while the average pore size of the carbons is absolutely decreased with the

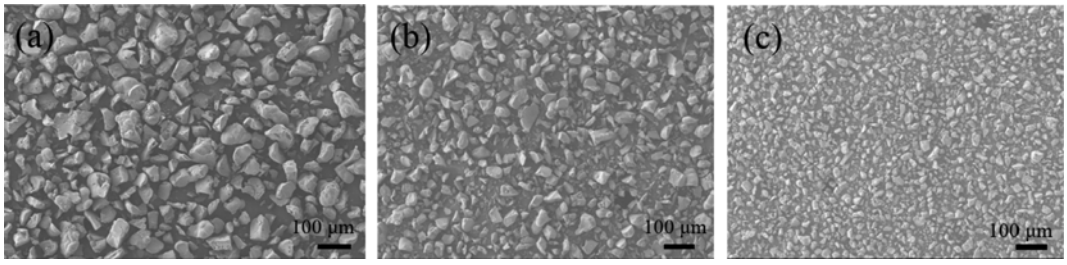

Fig. 2. SEM images of the mesoporous carbon catalysts (a) CNx-A, (b) CNx-B, and (c) CNx-C.

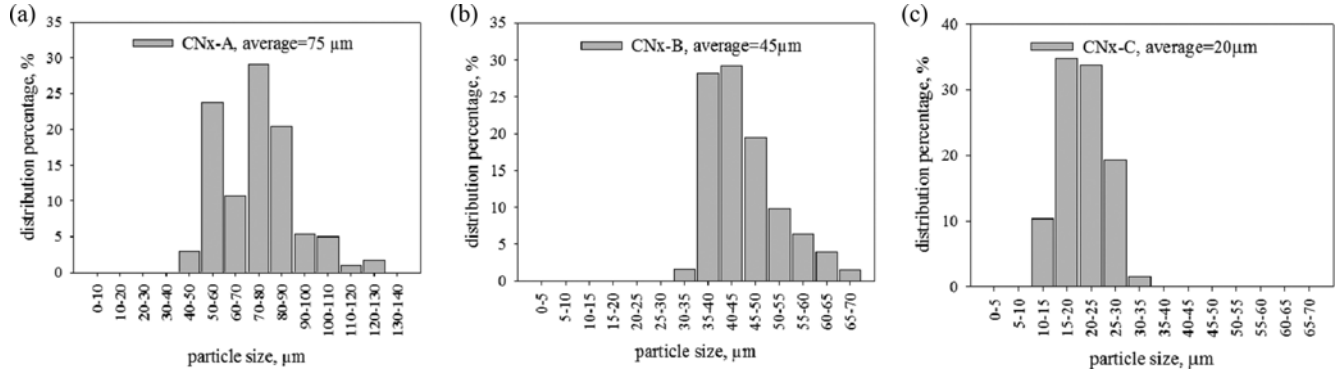

Fig. 3. Particle size distributions of N-doped mesoporous carbon catalysts (a) CNx-A, (b) CNx-B, and (c) CNx-C.

pore diameters of from 4.55 to 4.13 nm, as shown in Table 1. Dorjgotov et al. [33] discussed the pore size distribution of mesoporous carbon catalysts at the ORR activity. They discussed that the pore size and specific surface area, which are directly related to the mass transfer resistance and the number of active sites, are important factors for increasing the cell performance and catalyst activity. Therefore, the ORR activity on all the carbons with different surface area and pore sizes was determined by RDE in the case of particle size distribution of N-doped mesoporous carbons.

Basically, the three different carbons were promoted by 1.5% transition metal of Fe. Yeager [34] and Gouerec et al. [35] demonstrated that MeN4/MeN2 structures were completely decomposed after pyrolysis at temperatures above 800 °C. They proposed that transition metals (Fe or Co) may not be a part of the active site but rather may serve to facilitate the incorporation of nitrogen into the carbon matrix. It is probable that the presence of nitrogen may enhance the electron donor property of the carbon matrix [36], weakening the O-O bond via bonding between oxygen and nitrogen and/or the adjacent carbon atoms, thereby facilitating the ORR. There are some disagreements regarding the ORR active sites, and little is currently known about the stability of this carbon composite and its ability to survive in the operating conditions of PEMFCs [37]. Therefore, in this case transition metal promoted N-doped mesoporous carbons were prepared for ORR test. Previous studies suggested that the 1.5% Fe is a more effective activity on the N-doped mesoporous carbons.

To evaluate the effect of particle size distribution on ORR, Fig. 4 shows the polarization curves for oxygen reduction on the CNx-A 1.5% Fe-L-HT, CNx-B 1.5% Fe-L-HT and CNx-C 1.5% Fe-L-HT catalysts in O_2-saturated 0.5 M H_2SO_4 at room temperature, using a potential scan rate of 5 mV/s and a rotation rate of 1,600 rpm. In the case of all the N-mesoporous carbon catalysts, the carbon catalysts revealed a similar onset potential of about 0.8 V. There is a slight increase in the ORR activity from the dropping region while the particle size decreases. The number of active sites on the catalyst surface should be higher for catalyst with larger specific areas of the smaller CNx carbons. Interestingly, the diffusion current densities (mA/cm^2) were 4.21, 4.32 and 4.45 mA/cm^2 for CNx-A 1.5% Fe-L-HT, CNx-B 1.5% Fe-L-HT and CNx-C 1.5% Fe-L-HT at the lowest voltage of experiment, respectively. From the results of polarization curves of oxygen reduction, the mass transfer of the reactants increased much more with the smaller particle. This can be due to the higher surface area and pore volumes for the smaller CNx, which was earlier mentioned and closely related to the better pore configuration structure for the transferring and reacting by oxygen during the ORR tests.

The activity and mass transfer of the electrode were also confirmed by the CV analysis in the single cell test. The CV plots of the N-doped mesoporous carbon catalysts CNx-A 1.5% Fe-L-HT, CNx-B 1.5% Fe-L-HT and CNx-C 1.5% Fe-L-HT are shown in Fig. 5, with a sweep rate of 5 mV/s within the 0-1.2 V potential range. Interestingly, the relatively smaller particle size with a higher specific surface area is closely related to the catalyst properties. This definitely shows an improvement of the electrochemical property,

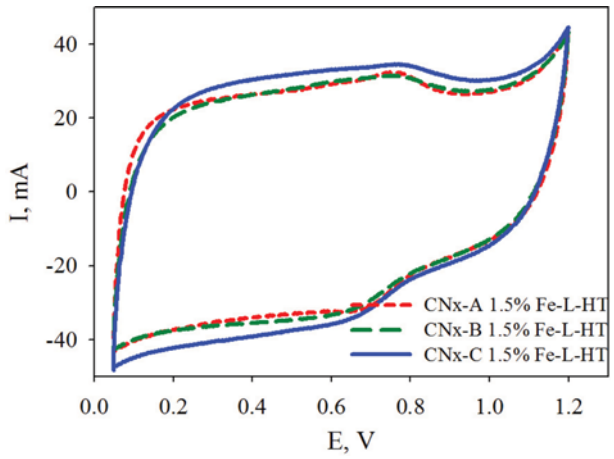

Fig. 5. Cyclic voltammetry (CV) curves of N-doped mesoporous carbon catalysts of CNx-A 1.5% Fe-L-HT, CNx-B 1.5% Fe-L-HT and CNx-C 1.5% Fe-L-HT.

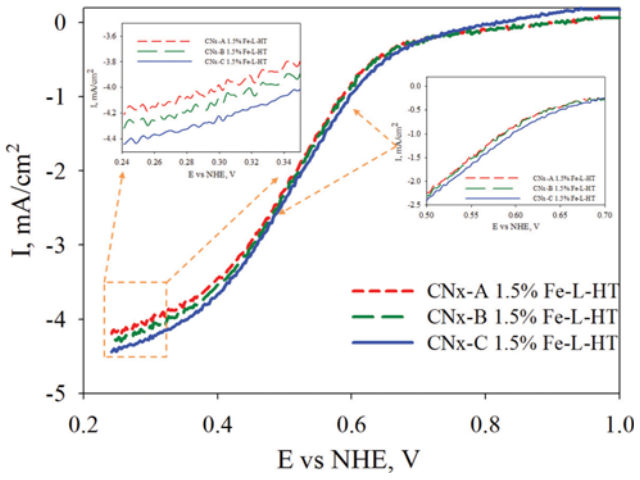

Fig. 4. Polarization curves of oxygen reduction for the N-doped mesoporous carbon catalysts of CNx-A 1.5% Fe-L-HT, CNx-B 1.5% Fe-L-HT and CNx-C 1.5% Fe-L-HT.

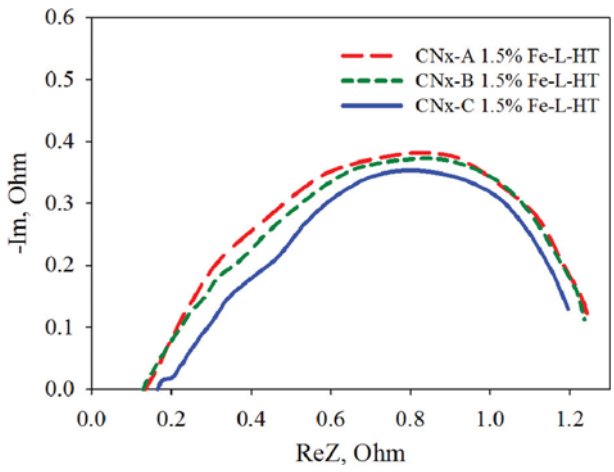

Fig. 6. Electrochemical impedance spectroscopy of N-doped mesoporous carbon catalysts of CNx-A 1.5% Fe-L-HT, CNx-B 1.5% Fe-L-HT and CNx-C 1.5% Fe-L-HT.

which may increase the PEMFC performance. It can thus be said that when the particle sizes were changed, ORR activity of carbon catalyst was increased due to higher amount of active sites from the higher surface area. To determine the particle size effect on the electrode resistance properties, the ohmic resistance (R_Ω) and charge transfer resistance (R_C) of the MEA were measured via electrochemical impedance spectroscopy (EIS). This was operated at a cell voltage of 0.6 V, as shown in Fig. 6. Generally, the R_Ω is obtained at a high-frequency region on the real axis of semicircles, and it is influenced by the ionic conductivity through the catalyst layer and membrane as combined with the polymer electrolyte, catalyst, and Nafion membrane in the MEA. The R_Ω values of the all of carbon cathode catalysts were ~0.12 Ω cm^2, respectively, due to the use of the same membrane. The R_C values of the carbon catalysts with different particle sizes were definitely reduced with the order of CNx-A 1.5% Fe-L-HT, CNx-B 1.5% Fe-L-HT and CNx-C 1.5% Fe-L-HT, respectively. These results confirm that the smaller particle size of the carbon catalyst XV the reduction of the charge transfer resistance for enhanced mass transfer of the reactants.

Overall, of these CV and impedance results, Fig. 7 shows the single cell test results of PEMFCs prepared with the CNx-A 1.5% Fe-L-HT, CNx-B 1.5% Fe-L-HT and CNx-C 1.5% Fe-L-HT cathode catalysts. The cathode catalyst loading is maintained 4.95 mg/cm^2. The experiments were performed without back pressure. Ohmic potential drop was not compensated in the measurements. As confirmed from the ORR activity, although, the polarization curves show same open circuit potentials of ~0.85 V for all the catalysts with three different particle sizes. There were also similar activation polarization losses with a current density 0.2 A/cm^2 at 0.5 V, which was hard to analyze the difference, but shows a slight increase. It indicates that the particle sizes according to the surface area influence obviously the catalytic activity for single cell operation. In this work, all the pore sizes were large enough for the mass transfer, but the smaller pore size provides higher surface area, which is also a crucial factor for better mass transfer. In the mass transfer region, differences were observed with an increase in the limited current densities by decreasing particle sizes and higher

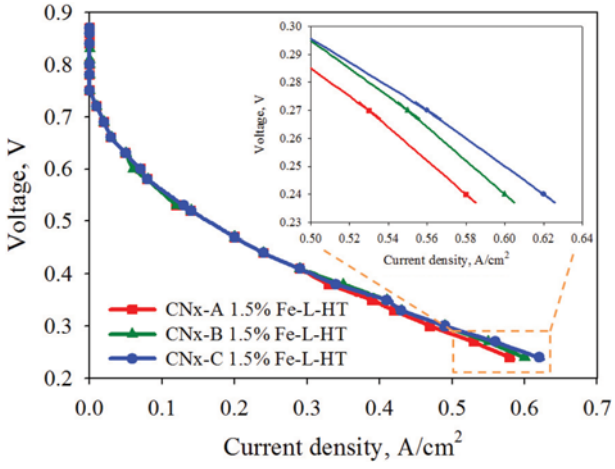

Fig. 7. Polarization curves of N-doped mesoporous carbon catalysts of CNx-A 1.5% Fe-L-HT, CNx-B 1.5% Fe-L-HT and CNx-C 1.5% Fe-L-HT.

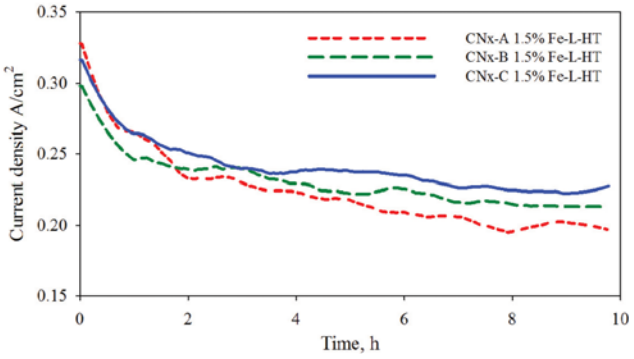

Fig. 8. Durability test of N-doped mesoporous carbon catalysts of CNx-A 1.5% Fe-L-HT, CNx-B 1.5% Fe-L-HT and CNx-C 1.5% Fe-L-HT.

surface area. It was related to the mass transfer resistance, which may reduce the loss of catalyst performance [31]. Therefore, it can be concluded that the higher surface area from smaller particles is an important factor for increased MEA performance. Fig. 8 shows the durability test behavior of the CNx carbons at 0.5 V. In this case, all of current densities decrease for the first 5 hours. Compared to the different size of the CNx carbons, the CNx-C carbon with a smaller size shows smaller reduction of its current density with a value of 0.09 A/cm^2 while the other carbons display reductions of 0.14 and 0.12 A/cm^2 for CNx-A and CNx-B, respectively, during 10 hours. However, then it was still stable after 10 hours, when the durability test was carried out, with a current density of around 0.2 A/cm^2 for all of carbon catalysts. While the particle size of carbon was becoming smaller, less stability loss occurred than the big particle sizes due to the better physical properties in the electrode for the MEA operation as mentioned before.

CONCLUSION

Three types of mesoporous silica different from each other by particle size were synthesized successfully. These silicas can be a very stable template for the synthesis of mesoporous nitrogen doped carbon. When the particle size decreased from 75 to 45 and 25 μm, the pore size was decreased and the surface area/pore volume obviously increased. At the decreasing carbon pore size for the smaller particles, a slightly higher activity on the ORR and MEA was observed due to the large surface area. Interestingly, at the mass transfer region in PEMFC, a difference of limited current density was observed, and current density increased at the decreasing of particle size with higher pore volume and smaller pore size in the carbons. From the durability test, all prepared cathode catalysts resulted in good stability after 10 hours, but carbon catalysts with decreasing the particle sizes of carbon were more stable even at early hours. Therefore, changing particle sizes did an effect to both activity and mass transfer, but more to the mass transfer with the same carbon catalyst for ORR and PEMFC.

REFERENCES

1. C. W. B. Bezerra, L. Zhang, K. Lee, H. Liu, A. L. B. Marques, E. P.

Marques, H. Wang and J. Zhang, *Electrochim. Acta*, **53**, 4937 (2008).
2. Y. Wei, C. Shengzhou and L. Weiming, *Int. J. Hydrogen Energy*, **37**, 942 (2012).
3. Z. Chen, D. Higgins, A. Yu, L. Zhang and J. Zhang, *Energy Environ. Sci.*, **4**, 3167 (2011).
4. R. Liu, D. Wu, X. Feng and K. Mullen, *Angew. Chem. Int. Ed.*, **49**, 2565 (2010).
5. G. Liu, X. Li, P. Ganesan and B. N. Popov, *Appl. Catal. B.*, **93**, 156 (2009)
6. D. Yu, E. Nagelli, F. Du and L. Dai, *J. Phys. Chem. Lett.*, **1**, 2165 (2010).
7. S.-T. Chang, H.-C. Hsu, H.-C. Huang, C.-H. Wang, H.-Y. Du, L.-C. Chen, J.-F. Lee and K.-H. Chen, *Int. J. Hydrogen Energy*, **13**, 13755 (2012).
8. H. S. Oh, J. G. Oh, W. H. Lee, H. J. Kim and H. Kim, *Int. J. Hydrogen Energy*, **36**, 8181 (2011).
9. C. Arbizzani, S. Righi, F. Soavi and M. Mastragostino, *Int. J. Hydrogen Energy*, **36**, 5038 (2011).
10. Y. Y. Shao, J. H. Sui, G. P. Yin and Y. Z. Gao, *Appl. Catal. B.*, **79**, 89 (2008).
11. S. Maldonado and K. J. Stevenson, *J. Phys. Chem. B.*, **109**, 4707 (2005).
12. S. V. Dommete, K. P. D. Jong and J. H. Bitter, *Chem. Commun.*, **48**, 59 (2006).
13. W. Wei, H. Liang, K. Parvez, X. Zhuang, X. Feng and K. Müllen, *Angew. Chem. Int Ed.*, **53**, 1570 (2014).
14. K. Gong, F. Du, Z. Xia, M. Durstock and L. Dai, *Science*, **323**, 760 (2009).
15. X. Yang, W. Zou, Y. Su, Y. Zhu, H. Jiang, J. Shen and C. Li, *J. Power Sources*, **266**, 36 (2014).
16. Z. Mo, R. Zheng, H. Peng, H. Liang and S. Liao, *J. Power Sources*, **245**, 801 (2014).
17. R. Liu, D. Wu, X. Feng and K. Mullen, *Angew. Chem. Int. Ed.*, **49**, 2565 (2010).
18. L. Zhang, Z. Su, F. Jiang, L. Yang, J. Qian, Y. Zhou, W. Li and M. Hong, *Nanoscale.*, **6**, 6590 (2014).
19. H. Jiang, Y. Zhu, Q. Feng, Y. Su, X. Yang and C. Li, *Chem.- Eur. J.*, **20**, 3106-12 (2014).
20. B. Fang, J. H. Kim, M. S. Kim and J. S. Yu, *Acc. Chem. Res.*, **46**, 1397 (2013).
21. R. W. Fu, Z. H. Li, Y. R. Liang, F. Li, F. Xu and D. C. Wu, *New Carbon Mater.*, **26**, 171 (2011).
22. R. Gokhale, S. M. Unni, D. Puthusseri, S. Kurungot and S. Ogale, *Phys. Chem. Chem. Phys.*,**16**, 4251 (2014).
23. J. Yan, H. Meng, F. Xie, X. Yuan, W. Yu, W. Lin, W. Ouyang and D. Yuan, *J. Power Sources*, **245**, 772 (2014).
24. A. H. A. Videla, L. Zhang, J. Kim, J. Zeng, C. Francia, J. Zhang and S. Specchia, *J. Appl. Electrochem.*, **43**, 159 (2013).
25. M. Lefèvre, E. Proietti, F. Jaouen and J. P. Dodelet, *Science*, **324**, 71 (2009).
26. G. Wu, K. L. More, C. M. Johnston and P. Zelenay, *Science*, **332**, 443 (2011).
27. P. H. Matter, E. Wang, M. Arias, E. J. Biddinger and U. S. Ozkan, *J. Mol. Catal. A: Chem.*, **264**, 73 (2007).
28. Y. Tan, C. Xu, G. Chen, X. Fang, N. Zheng and Q. Xie, *Adv. Funct. Mater.*, **22**, 4584 (2012).
29. M. Lefevre, J. P. Dodelet and P. Bertrand, *J. Phys. Chem. B.*, **104**, 11238 (2000).
30. P. H. Matter, E. Wang and U. S. Ozkan, *J. Catal.*, **243**, 395 (2006).
31. C. Portet, G. Yushin and Y. Gogotsi, *J. Electrochem. Soc.*, **155**, A531 (2008).
32. A. Katiyar, S. Yadav, P. G. Smirniotis and N. G. Pinto, *J. Chromatogr. A.*, **1122**, 13 (2006).
33. A. Dorjgotov, J. H. Ok, Y. W. Jeon, S. H. Yoon and Y. G. Shul, *J. Solid. State. Electrochem.*, **17**, 2567 (2013).
34. E. Yeager, *Electrochim. Acta.*, **29**, 1527 (1984).
35. P. Gouerec, M. Savy and J. Riga, *Electrochim. Acta*, **43**, 743 (1997).
36. S. Kundu, T. C. Nagaiah, W. Xia, Y. Wang, S. V. Dommele, J. H. Bitter, M. Santa, G. Grundmeier, M. Bron, W. Schuhmann and M. Muhler, *J. Phys. Chem. C.*, **113**, 14302 (2009).
37. H. A. Gasteiger and N. M. Markovic, *Science*, **324**, 48 (2009).